Bioorganic & Medicinal Chemistry Letters 22 (2012) 2565–2571

Contents lists available at SciVerse ScienceDirect

Bioorganic & Medicinal Chemistry Letters

journal homepage: www.elsevier.com/locate/bmcl

# Discovery of P2X3 selective antagonists for the treatment of chronic pain

Louis-David Cantin [a,*], Malken Bayrakdarian [a], Christophe Buon [a], Eric Grazzini [c], Yun-Jin Hu [a], Jean Labrecque [c], Carmen Leung [a], Xuehong Luo [a], Giovanni Martino [c], Michel Paré [c], Kemal Payza [c], Nirvana Popovic [a], Denis Projean [b], V. Santhakumar [a], Christopher Walpole [a], Xiao Hong Yu [c], Mirosław J. Tomaszewski [a]

[a] Department of Medicinal Chemistry, AstraZeneca R&D, 7171 Frederick-Banting, Montréal, QC, Canada H4S 1Z9
[b] Department of Drug Metabolism and Pharmacokinetics, AstraZeneca R&D, 7171 Frederick-Banting, Montréal, QC, Canada H4S 1Z9
[c] Department of Biosciences, AstraZeneca R&D, 7171 Frederick-Banting, Montréal, QC, Canada H4S 1Z9

ARTICLE INFO

*Article history:*
Received 16 December 2011
Revised 27 January 2012
Accepted 30 January 2012
Available online 9 February 2012

*Keywords:*
P2X3
Purinergic receptors
Analgesia
Pyrrolo-pyrimidinones
Nociceptive pain

ABSTRACT

Purinergic receptor P2X3 has been linked to analgesia in a number of pre-clinical models of pain, and is expressed in the human pain perception pathway. Only few P2X3-selective antagonists have been reported to date. This Letter describes the SAR and in vivo analgesic profile of a novel scaffold of selective P2X3 antagonists.



Chronic pain can erode the quality of life of patients suffering from conditions such as arthritis. Additionally peripheral nerve damage caused by complications of diseases such as diabetes, viral infections or cancer can also evolve into chronic neuropathic pain. While current treatments can offer some pain relief, patients often become non-responsive to these therapies, or need to bear with incapacitating side-effects.[1] For example, patients suffering from osteoarthritis may only get partial pain relief from non-steroidal anti-inflammatory drugs, while experiencing side-effects that range from gastro-intestinal discomfort to ulcers, renal failure and increased risks of myocardial infarction.

Seminal work of Burnstock[2] and North[3] has elucidated the role of purinergic receptors in disease conditions and highlighted their potential value in the development of novel therapeutics. Purinergic receptors are classified into two sub-families: P2Y receptors that are GPCRs, and P2X receptors that are ligand-gated ion channels for which the endogenous ligand is ATP. The conserved expression of P2X3 in the pain pathways (including dorsal root and trigeminal ganglia)[4] made this an attractive target for our research team.

The P2X3 receptor is a homomeric trimer assembled from three P2X3 monomers. Two units of P2X3 monomer can also form heteromeric trimers when combined with one P2X2 monomer, leading to the P2X2/3 receptor.[5] The latter has some overlapping expression with P2X3 receptor, complicating the assessment of the role of P2X3 in vivo. Despite having access to P2X3 and P2X2 knock-out animals, understanding the relative contributions of P2X3 and P2X2/3 to pain perception has been difficult since knock-out animals lack both the homomer and heteromer.[6] Initial reports from an Abbott research group on the use of A-317491 (**1**, Fig. 1) allowed for the characterization of unselective antagonists as efficacious analgesic in pre-clinical models of pain.[7]

Subsequent reports from Roche,[8] confirmed the role of P2X3–P2X2/3 and disclosed the first orally active compounds (**2**, **3**).[9] Only recently have reports of antagonists selective for P2X3 been published (**4**), but the in vivo efficacy data has yet to be shared.[10] Therefore, it remains unclear whether the analgesic effects seen with P2X3 antagonists require blockade of P2X3 homotrimers or P2X2/3 heterotrimers, or both. This Letter will discuss SAR exploration and in vivo characterization of a novel scaffold for P2X3-selective antagonists.

With the goal of identifying orally available P2X3 antagonists, we explored a variety of hit-finding options. Lacking meaningful structural information about the target, we decided to undertake an HTS screen,[11] in which 800,000 compounds were assayed. This

* Corresponding author.
*E-mail addresses:* Louis-david.cantin@astrazeneca.com, ldcantin@eckerdalumni.com (L.-D. Cantin).

0960-894X/$ - see front matter © 2012 Elsevier Ltd. All rights reserved.
doi:10.1016/j.bmcl.2012.01.124

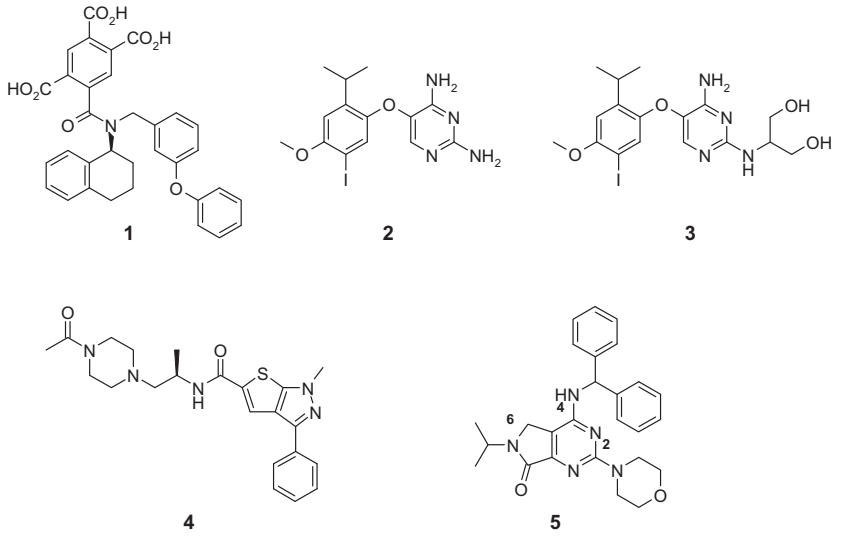


**Figure 1.** Antagonists of P2X3 and P2X2/3.

approach led to the identification of 445 hits, from which a small cluster of pyrrolo-pyrimidinones was identified. For example, compound **5** ( Fig. 1) displayed promising potency at hP2X3 ($IC_{50}$, 1.3 μM), however the high lipophilicity ($\log D_{7.4}$ 4.3) and low aqueous solubility (pH 7.4, 1 μM) presented areas for improvements.

Synthesis[12] of the desired analogs began with condensation of orotic acid (**6**, Scheme 1) with paraformaldehyde to give the corresponding lactone **7**, which was in turn converted to the dichloropyrimidine intermediate **8**. Introduction of phenylbenzylamine occurred chemoselectively at the C4 position under mild conditions to provide **9**, an advanced intermediate ready for further derivatization. The C2 substituent was introduced by reacting chloro **9** with the appropriate amine in *n*-butanol at 140 °C. Subsequent lactam formation under more forcing conditions (195 °C) afforded compounds **11a–h**, albeit in low yield.

Our initial exploration of the lactam substituent ($R^3$) showed that this section of the molecule was intolerant to modifications; the original isopropyl group provided the best potency (data not shown). The C2 position provided more opportunities to introduce structurally diverse substituents (Table 1). For example, the morpholine group could be replaced by a piperazine (**11a**) without affecting potency, but dramatically improving solubility. A smaller pyrrolidine **11b** was also well tolerated, as was the opening of the morpholine ring (**11c**). However, in both cases solubility was not improved relative to that of **11a**. Wanting to retain rigidity in this section of the molecule, we decided to explore the piperazine group further. Methylation of the piperazine (**11d**) caused a fourfold decrease in potency with a slight improvement in solubility. However, for both **11a** and **11d**, the basic nature of the compounds raised concerns with their eventual safety profile (e.g., risks to encounter PLD, hERG inhibition). Introduction of an acetyl group (**11e**) increased potency twofold while reducing the $pK_a$. A sulfonamide group (**11f**) was also well tolerated, as was the *N,N*-dimethyl-proprionamide group (**11g**). However, using an *N,N*-dimethylamino acetyl group (**11h**) caused a 10-fold decrease in potency indicating that a charged group was not tolerated.

This initial exploration of the SAR provided us with **11e**, a compound with sufficient potency to reliably assess selectivity over the heteromer. Compound **11e** proved very selective against rat P2X2/3, with an $IC_{50}$ >2.5 μM. This level of selectivity should enable us to

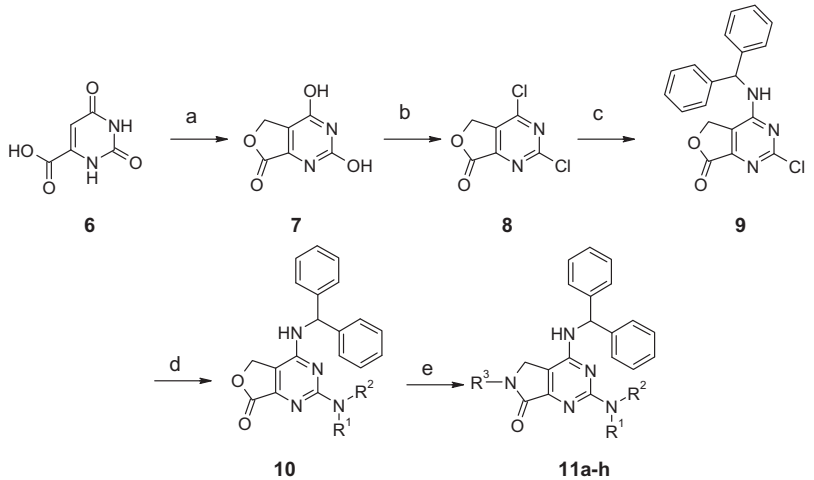


**Scheme 1.** Synthesis of pyrrolo-pyrimidinones through late-stage lactam formation. Reagents and conditions: (a) $(CH_2O)_2$, HCl, 85–95 °C, 77% yield; (b) $POCl_3$, *N,N*-diethylaniline, 110 °C, 98% yield; (c) phenylbenzylamine, DIPEA, $CH_2Cl_2$, rt, 47% yield. d) $R^1R^2NH$, *n*-butanol, 140 °C, 53–61% yield; (e) $R^3NH$, HCl, methoxymethanol, 195 °C, 8–23% yield.

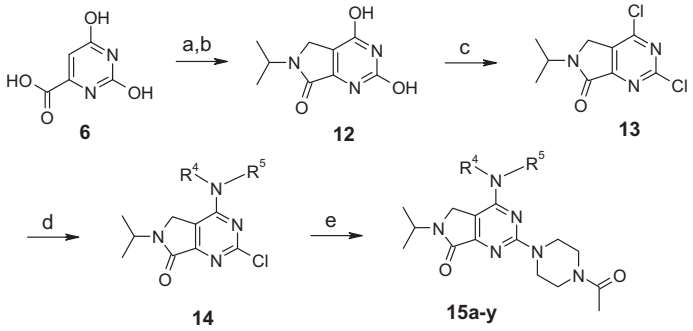


**Scheme 2.** Synthesis of pyrrolo-pyrimidinones through Mannich-type condensation. Reagents and conditions: (a) *i*-$PrNH_2$, $(CHO)_n$, ethanol, reflux; (b) methoxyethanol, reflux, 70% yield (over two steps); (c) $POCl_3$, *N*,*N*-diethylaniline, 110 °C, 65% yield; (d) $R^1R^2NH$, DIPEA, $CH_2Cl_2$, rt; (e) acetylpiperazine, *n*-butanol, 160 °C, microwave reactor, 70–90% yield over two steps.

**Table 1**
Exploration of the C2 position of the pyrrolo-pyrimidinone scaffold ($R^3$ = *i*-Pr)

| Ex | $NR^1R^2$ | hP2X3[a] ($IC_{50}$) | Solubility[b] (pH7.4, μM) |
|---|---|---|---|
| **5** | 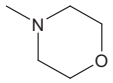 | 1360 | <1 |
| **11a** | 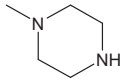 | 618 | 1000 |
| **11b** | 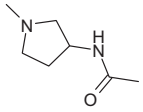 | 327 | <1 |
| **11c** | 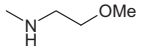 | 255 | <1 |
| **11d** | 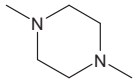 | 1947 | 7 |
| **11e** | 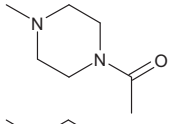 | 268 | <1 |
| **11f** | 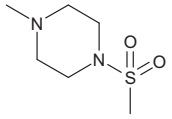 | 398 | <1 |
| **11g** | 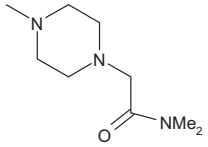 | 440 | 3.5 |
| **11h** | 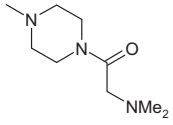 | 5689 | 50 |

[a] FLIPR®, mean $IC_{50}$ hP2X3, RLE cells loaded with FLUO-2 and stimulated with 100 μM (α,β)me-ATP; $IC_{50}$ values are the mean of at least three experiments performed in triplicates, with a SD of ±20%.

[b] Thermodynamic solubility measured in a pH 7.4 buffer using HPLC with UV detection for quantification.

obtain an unambiguous assessment of analgesic potential of P2X3-selective compounds. However, compound **11e** still suffered from poor solubility, despite having lower lipophilicity relative to **5**. Improving aqueous solubility therefore became a focus for the design of future analogs during our exploration of the SAR at the C4-position.

Having identified suitable substituents at the 2- and 6-positions of the pyrrolo-pyrimidinone core, we decided devise of a more efficient synthetic route. Introduction of the isopropyl group at the 6-position was achieved through a Mannich-type condensation between orotic acid **6**, formaldehyde and isopropylamine; subsequent lactam formation to produced **12**. Careful control of the reaction conditions allowed us to selectively chlorinate the C2- and C4-positions using $POCl_3$, without affecting the lactam. With **13** in hand, we were poised to explore the C4 position. Reaction of selected amines with **14** under mild conditions, followed by introduction of the acetyl piperazine moiety provided compounds **15a–w** in good yield for a wide variety of compounds.

We began our exploration of the C4 group ($NR^4R^5$) by removing one of the aromatic rings (**15a**, Table 2), which resulted in a more soluble yet inactive compound.

Lengthening the substituent by one methylene unit (**15b**) provided marginal antagonism, which was only improved by the addition of lipophilic substituents to the aromatic ring. Indeed, either a 4-Cl (**15c**) or a 4-Me (**15d**) group provided compounds with micromolar potency and measurable aqueous solubility. Restoring lipophilicity in the linker area increased potency, as exemplified by the methyl-substituted compound (**15e**). However, adding a second methyl group (**15f**) erased this gain in potency. Surprisingly, using a cyclobutyl group (**15g**) restored potency while moving the *gem*-dimethyl group close to the C4-amino group (**15h**) provided the most potent compound yet.

Despite having poor aqueous solubility and poor stability in rat liver microsomes (rCLint 83 μL/min/mg), we seized the opportunity to profile **15h** in our pre-clinical models of pain to ascertain the contribution of P2X3 antagonism to analgesia. While **15h** shows a slight decrease in potency at rat P2X3 ($IC_{50}$ 280 nM) compared to human P2X3, this compound shows a greater than 10-fold selectivity against rat P2X2/3 ($IC_{50}$ >2.5 μM, FLIPR)[13] and was devoid of activity against a panel of more than 200 targets. Following subcutaneous administration of **15h**, we observed an analgesic effect (Fig. 2a) that was dose responsive in a model of chronic nociceptive pain (FCA-treated rats).[14]

Analysis of the plasma concentration-response relationship revealed an $EC_{50}$ of 199 nM (free plasma concentration, $E_{max}$ = 90%) in-line with the in vitro $IC_{50}$ of **15h**. Further, the plasma levels remained well below the in vitro $IC_{50}$ of **15h** against P2X2/3, suggesting that the observed efficacy was due solely to antagonism of P2X3. Given the low free brain exposure levels of **15h** in rats (Br/Pl = 0.02, unbound fraction in brain homogenate ~3%), we postulated that there would not be significant central contribution to the analgesic effects we observed. To investigate this hypothesis

**Table 2**
Exploration of the C4 position of the pyrrolo-pyrimidinone scaffold

| Ex | $NR^4R^5$ | hP2X3[a] ($IC_{50}$) | Solubility[b] (μM) |
|---|---|---|---|
| **11e** | 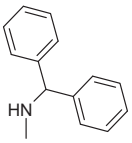 | 268 | <1 |
| **15a** | 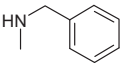 | >30,000 | 230 |
| **15b** | 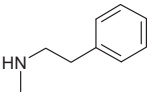 | 13,950 | 140 |
| **15c** | 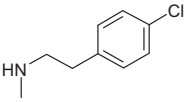 | 1665 | 28 |
| **15d** | 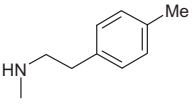 | 1311 | 28 |
| **15e** | 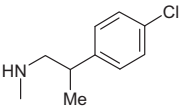 | 441 | 32 |
| **15f** | 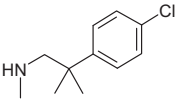 | 2057 | 12 |
| **15g** | 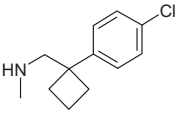 | 262 | 46 |
| **15h** | 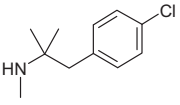 | 61 | 24 |

[a] FLIPR®, mean $IC_{50}$ hP2X3, RLE cells loaded with FLUO-2 and stimulated with 100 μM (α,β)me-ATP; $IC_{50}$ values are the mean of at least three experiments performed in triplicates, with a SD of ±20%.
[b] Thermodynamic solubility measured in a pH 7.4 buffer using HPLC with UV detection for quantification.

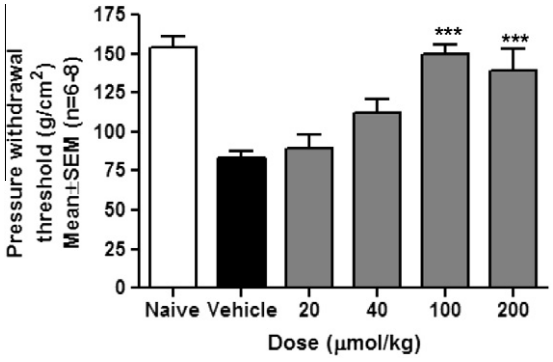


**Figure 2a.** Analgesic effects of **15h** in the 96h FCA rat model upon sc dosing.

further, we administered **15h** via an intrathecal route to FCA-treated rats, which did not produce any analgesic effects. Differently, intraplantar administration of similar doses of **15h** produced significant analgesic effects (Fig. 2b). Taken together, these results allowed us to more clearly chart a path forward in our drug

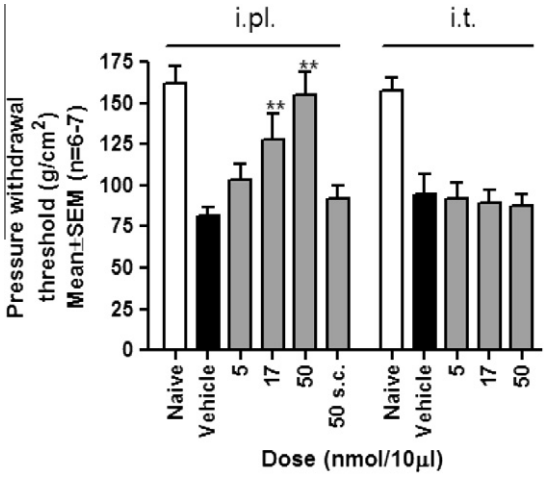


**Figure 2b.** Analgesic effects of **15h** in the 96h FCA rat model upon ip and it dosing.

discovery work to identify P2X3-selective compounds that would not require necessarily high CNS exposure.

Having clarified the site of action and demonstrated that a P2X3-selective compound could produce robust analgesic effects, we continued our exploration of the lead series. Profiling **15h** further revealed that improvements in physicochemical and DMPK properties (e.g., in vitro metabolic stability, in vivo clearance) were still needed, and that CYP2C9 inhibition ($IC_{50}$ 2 μM) required improvement.

We therefore decided to re-investigate the C4 benzyl substituent by introducing structurally diverse substituents to modulate electronic properties. Adding a lipophilic group such as Cl (**15i**, Table 3) increased potency, which was further enhanced by using more electron withdrawing groups such as trifluoromethyl (**15j**) and trifluoromethoxy (**15k**). Indeed, compound **15k** combined promising potency with good stability in human liver microsomes (hCLint) and acceptable solubility. The addition of an electron donating group at the *ortho*-position (**15l**) produced a substantial improvement in potency; however solubility and microsomal stability decreased. We decided to apply the lessons learned from the C4-homobenzyl amine SAR and introduced a small substituent in the methylene α to the nitrogen. We observed that an *S*-methyl group[15] (**15m**) provided an eightfold increase in potency. Combination of the α-methyl with other 4-subtituents revealed interesting SAR. Indeed, a methyl substituent (**15m**) was substantially less potent than the corresponding trifluoromethoxy group (**15n**) as was the methoxy group (**15o**); however an ethoxy group proved most potent (**15p**). Having lowered lipophilicity ($\log D_{7.4}$ 3.0) relative to **15e**, **15p** showed substantially improved solubility and stability in human microsomes. The CYP inhibition profile was also improved over previous analogs; however compound **15p** only showed moderate permeability in the Caco-2 assay. Further assessment revealed that this compound suffered from significant efflux in Caco-2 cells and was a substrate of a drug transporter, P-glycoprotein. Inhibition studies with a P-gp inhibitor (quinidine) in Caco-2 cells further confirmed that this mechanism was responsible in limiting its in vitro permeability.

We thus decided to continue exploring the SAR with a focus on increasing permeability without affecting the overall profile of **15p** through small structural modifications. Using an α-ethyl (**15q**) or an α-$CF_3$ (**15r**) group resulted in substantial decreases in potency and no gains in permeability. Addition of substituents on the aryl ring, as exemplified by **15s**, was tolerated, but led to an erosion of microsomal stability. Replacing the phenyl ring by a pyridine (**15t**) led to a 15-fold drop in potency, whereas extension of the

**Table 3**
Exploration of the C4 position of the pyrrolo-pyrimidinone scaffold

| Ex | $NR^4R^5$ | hP2X3[a] ($IC_{50}$, nM) | Sol.[b] (μM) | hCLint[c] (μL/min/mg) | CYP2C9[d] ($IC_{50}$, μM) | Caco-2[e] (1E-6 cm/s) |
|---|---|---|---|---|---|---|
| **15i** | 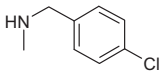 | 4214 | 30 | 6 | 2.4 | |
| **15j** | 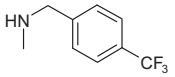 | 1271 | 17 | 31 | | |
| **15k** | 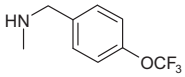 | 324 | 84 | 4 | 2.4 | 2.9 |
| **15l** | 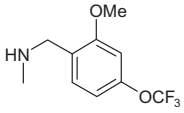 | 67 | 10 | 31 | | |
| **15m** | 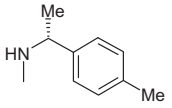 | 613 | 260 | | | |
| **15n** | 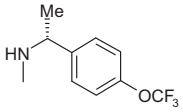 | 64 | 61 | 22 | 7.3 | 4.5 |
| **15o** | 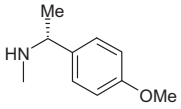 | 2523 | 84 | 4 | 2.4 | |
| **15p** | 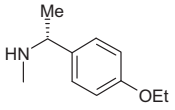 | 69 | 120 | 10 | >10 | 2.4 |
| **15q** | 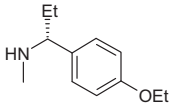 | 212 | 86 | 10 | | |
| **15r** | 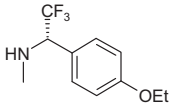 | 115 | 72 | 5 | 14 | 2 |
| **15s** | 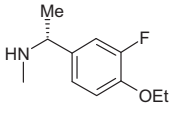 | 38 | 220 | 17 | 11 | 0.8 |
| **15t** | 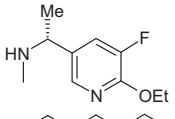 | 521 | 58 | 7 | | |
| **15u** | 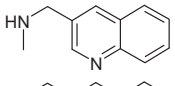 | 24 | 3 | 11 | 16 | 0.1 |
| **15v** | 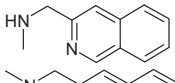 | 24 | 590 | 16 | 7 | 0.6 |
| **15w** | 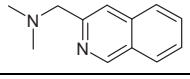 | 22 | 1100 | 19 | 7 | 2.9 |

[a] FLIPR®, mean $IC_{50}$ hP2X3, RLE cells loaded with FLUO-2 and stimulated with 100 μM (α,β)me-ATP; $IC_{50}$ values are the mean of at least three experiments performed in triplicates, with a SD of ±20%.
[b] Thermodynamic solubility measured in a pH 7.4 buffer using HPLC with UV detection for quantification.
[c] Metabolic stability performed in human liver microsomes in presence of NADPH using test compound at 1 μM.
[d] P450 inhibition screen using recombinant CYP2C9 and a fluorescent probe; $IC_{50}$ values are the mean of at least three experiments performed in duplicates, with a SD of ±20%.
[e] Transwell assay. Apparent permeability (apical to basolateral) across a caco-2 cell monolayer measured under pH gradient pH 6.5–7.4 using test compound at 10 μM applied on the apical side.

ring system to a quinoline (**15u**) led to one of the most potent compounds in this series. CYP2C9 inhibition was also improved and hCLint was in a favorable range, however solubility and permeability were poor. Using an isomeric isoquinoline (**15v**) increased sol-

**Table 4**
Pharmacokinetic profile of compounds **15h** and **15p**

| Ex | Dose (μm/kg) | $C_{max}$ (μM) | AUC (μM h) | $T_{1/2}$ (h) | CL[b] (ml/min/kg) | $F$(%) (oral) |
|---|---|---|---|---|---|---|
| **15h** (iv, rat) | 2.2 | — | 0.7 | 0.9 | 54 | |
| **15h** (sc, rat) | 5.9 | 1.0 | 2.8 | | | |
| **15p** (iv, rat) | 2.2 | — | 0.4 | 0.5 | 88 | |
| **15p** (iv, rat) | 11 | — | 8.05 | 2 | 22 | |
| **15p** (po, rat) | 12 | 0.1 | 0.4 | | | 16%[a] |
| **15p** (po, rat) | 58 | 6.9 | 1.8 | | | 62%[a] |
| **15p** (iv, dog) | 2.2 | — | 4.8 | 14.5 | 8 | |

[a] Calculated using the 2.2 μmol/kg iv dose.
[b] Rat liver blood flow = 72 mL/min/kg; dog liver blood flow = 55 mL/min/kg.

ubility substantially, however permeability remained unimproved. We speculated that removing the hydrogen bond donor NH would lead to an increase in permeability, which proved to be the case for the N-Me substituent (**15w**). However, decreased microsomal stability prevented further progression of these compounds.

Despite its moderate permeability, **15q** showed a balanced DMPK profile and we had confidence in achieving good oral exposure (rCLint 58 μl/min/mg; 60% rat liver blood flow). We decided to progress it into in vivo DMPK and into in vivo pre-clinical models chronic pain.

When administered to rats, (Table 4), the compound showed high systemic clearance (higher than the rat liver blood flow), short half-life and low oral bioavailability. The high clearance could not be explained completely by the measured in vitro metabolism either in rat microsomes (rCLint 17 μL/min/mg; 60% rat liver blood flow) or in rat hepatocytes. Because **15p** bears an amide function we speculated that this compound may be hydrolyzed in plasma, which proved not to be the case. Additionally, no preferential distribution was found in blood cells and therefore could not explain the observed discrepancy. Further exploration of the clearance mechanism revealed that only very small amounts of parent compound were recovered unchanged in rat urine, however a significant amount could be found in feces (>15% of the dose). Administration of higher doses intravenously led both to a decrease in plasma clearance and excretion in feces (<3% of the dose). Similarly, a higher oral dose led to an increase in bioavailability. Taken together, these results suggest that metabolism and additional saturable mechanisms (e.g., efflux in bile, secretion directly from blood to the gut mucosa) are involved in the disposition of this molecule in rat.

The physicochemical attributes of **15p**, combined with the fact that the compound is a substrate of drug transporters (P-gp), likely explains some of these unusual findings.[16] Interestingly, this phenomenon did not carry in higher species like the dog, where compound showed a lower clearance, in-line with the measured metabolic stability in dog hepatocytes (2.5 μL/min/$10^6$ cells, 20% liver blood flow).

Despite possessing an overall favorable in vitro selectivity profile (including against a panel of 100 targets) and suitable PK properties, the observation of compound-related (reversible) side-effects when tested in animals at higher doses precluded further progression of **15p** and its use as a tool compound. Indeed, in contrast to **15h**, **15p** displayed side-effects that prevented accurate measure of analgesic effects in behavior-based pre-clinical models of pain.

In summary, we have described our work in developing structurally novel P2X3-selective antagonists based on a pyrrolo-pyrimidinone core. Starting from a weakly active hit with poor physicochemical properties, we identified areas of the molecule useful to increase potency and improve physicochemical properties, while improving permeability and reducing CYP2C9 inhibition. This series of compounds provided us with useful tools, such as (**15h**), that demonstrated that analgesic effects, in the rat FCA model, of small molecule antagonists selective for P2X3 and added further support for a peripheral site of action in this model.

## Acknowledgments

The authors would like to recognize the contributions of Joanne Butterworth, Angelo Filosa, Claude Godbout, Vincent Kennedy, Giuseppe Molinaro Julie Pelland, Stéphane St-Onge, Pascal Turcotte and Huy Khang Vu to this work.

## References and notes

1. (a) Turk, D. C.; Wilson, H. D.; Cahana, A. *Lancet* **2011**, *377*, 2226; (b) Portenoy, R. K. *Lancet* **2011**, *377*, 2236.
2. Chen, C. C.; Akopian, A. N.; Sylviotti, L.; Colquhoun, D.; Burnstock, G.; Wood, J. N. *Nature* **1995**, *377*, 428.
3. Lewis, C.; Neidhart, S.; Holy, C.; North, R. A.; Buell, G.; Surprenant, A. *Nature* **1995**, *377*, 432.
4. Vulchanova, L.; Reidl, M. S.; Shuster, S. J.; Buell, G.; Suprenant, A.; North, R. A.; Elde, R. *Neuropharmacology* **1997**, *36*, 1229; (b) Xu, G. Y.; Huang, L. Y. *J. Neurosci.* **2002**, *22*, 93; (c) Chen, Y.; Li, G. W.; Wang, C.; Gu, Y.; Huang, L. Y. *Pain* **2005**, *119*, 38.
5. (a) North, R. A. *Curr. Opin. Cell Biol.* **1996**, *8*, 474; Virginio, C.; Robertson, G.; Surprenant, A.; North, R. A. *Mol. Pharmacol.* **1998**, *53*, 969.
6. (a) Honore, P.; Kage, K.; Mikusa, J.; Watt, A. T.; Johnston, J. F.; Wyatt, J. R.; Faltynek, C. R.; Jarvis, M. F.; Lynch, K. *Pain* **2002**, *99*, 11; Cockayne, D. A.; Hamilton, S. G.; Zhu, Q. M.; Dunn, P. M.; Zhong, Y.; Novakovic, S.; Malmberg, A. B.; Cain, G.; Berson, A.; Kassotakis, L.; Hedley, L.; Lachnit, W. G.; Burnstock, G.; McMahon, S. B.; Ford, A. P. *Nature* **2000**, *407*, 1011; (c) Cockayne, D. A.; Dunn, P. M.; Zhong, Y.; Rong, W.; Hamilton, S. G.; Knight, G. E.; Ruan, H. Z.; Ma, B.; Yip, P.; Nunn, P.; McMahon, S. B.; Burnstock, G.; Ford, A. P. *J. Physiol.* **2005**, *567*, 621; (d) Souslova, V.; Cesare, P.; Ding, Y.; Akopian, A. N.; Stanfa, L.; Suzuki, R.; Carpenter, K.; Dickenson, A.; Boyce, S.; Hill, R.; Nebenius-Oosthuizen, D.; Smith, A. J. H.; Kidd, E. J.; Wood, J. N. *Nature* **2000**, *407*, 1015.
7. (a) Jarvis, M. F.; Burgard, E. C.; McGaraughty, S.; Honore, P.; Lynch, K.; Brennan, T. J.; Subieta, A.; van Biesen, T.; Cartmell, J.; Bianchi, B.; Niforatos, W.; Kage, K.; Yu, H. X.; Mikusa, J.; Wismer, C. T.; Zhu, C. Z.; Chu, K.; Lee, C. H.; Stewart, A. O.; Polakowski, J.; Cox, B. F.; Kowaluk, E.; Williams, M.; Sullivan, J.; Faltynek, C. *Proc. Natl. Acad. Sci. U.S.A.* **2002**, *99*, 17179; (b) McGaraughty, S.; Wismer, C. T.; Zhu, C. Z.; Mikusa, J.; Honore, P.; Chu, K. L.; Lee, C.; Faltynek, C. R.; Jarvis, M. F. *Br. J. Pharmacol.* **2003**, *140*, 1381.
8. Ford, A.P. Purinergic Signalling, published online 18 Nov. 2011 (DOI 10.1007/s11302-011-9271-6).
9. (a) Carter, D. S.; Alam, M.; Cai, H. Y.; Dillon, M. P.; Ford, A. P. D. W.; Gever, J. R.; Jahangir, A.; Lin, C.; Moore, A. G.; Wagner, P. J.; Zhai, Y. S. *Bioorg. Med. Chem. Lett.* **2009**, *19*, 1628; (b) Gever, J. R.; Soto, R.; Henningsen, R. A.; Martin, R. S.; Hackos, D. H.; Panicker, S.; Rubas, W.; Oglesby, I. B.; Dillon, M. P.; Milla, M. E.; Burnstock, G.; Ford, A. P. *Br. J. Pharmacol.* **2010**, *160*, 1387; (d) Jahangir, A.; Alam, M.; Carter, D. S.; Dillon, M. P.; Du Bois, D. J.; Ford, A. P. D. W.; Gever, J. R.; Lin, C.; Wagner, P. J.; Zhai, Y. S.; Zira, J. *Bioorg. Med. Chem. Lett.* **2009**, *19*, 1632.
10. Brotherton-Pleiss, C. E.; Dillon, M. P.; Ford, A. P. D. W.; Gever, J. R.; Carter, D. S.; Gleason, S. K.; Lin, C. J.; Moore, A. G.; Thompson, A. W.; Villa, M.; Zhai, Y. *Bioorg. Med. Chem. Lett.* **2010**, *20*, 1031.
11. HTS assay measured inhibition of the increase in intracellular calcium induced by (α,β)-Me-ATP in cells expressing human P2X3.
12. Synthetic procedures and characterization data can be found in the following patent application: Bayrakdarian, M.; Buon, C.; Cantin, L.-D.; Hu, Y.-J.; Luo, X.;

Santhakumar, V.; Tomaszewski, M.J. WO2008136756. Some of the compounds can be prepared either using the route described in Scheme 1 or Scheme 2.

13. **15h** is a P2X3 antagonist non-competitive with (α,β)-Me-ATP. Data in the FLIPR assays is consistent with that generated using PatchXpress or manual patch clamp experiments using either cells overexpressing P2X3 or native rodent tissues.
14. Methods for characterization of analgesic effects of compounds in the 96h FCA rat model:
*Animals*: The animal experiments were approved by the AstraZeneca Animal Care Committee and were conducted in accordance with the guidelines provided by the Canadian Council on Animal Care and the Association for the Assessment and Accreditation of Laboratory Animal Care. Male Sprague–Dawley rats (Charles River, St-Constant, Qc, CAN) weighing 200–225 g were utilized for the animal experiment studies. The animals were group-housed in polycarbonate, ventilated cages (filter top) in a controlled environment room (12-h light/dark cycle, 20.5–23.5 °C, relative humidity: 40–70%) with food (14% Protein Rodent Maintenance Diet, Harlan Teklad, Madisson, WI, USA) and water ad libidum.
*Inflammatory pain model*: Inflammation was induced by injection of a single 40 μl Freund's complete adjuvant (FCA) intra-plantar injection into the rat's left hindpaw. All experiments were conducted 96h after FCA administration. Animals were sacrificed immediately after data acquisition.
*Behavioral measurements of nociception*: Twenty-four hours prior to behavioral testing animals were brought to the laboratory for acclimatization to the new environment. Mechanical hyperalgesia was assessed using the Ugo Basile analgesy meter (Ugo Basile, Comerio, Italy). Animals were gently restrained, and a steadily increasing pressure was applied to the dorsal surface of a hind paw via a probe with a dome-shaped tip (diameter of 1 mm). The pressure required to elicit paw withdrawal was determined. An assay cut off was set at 295 g. Two trials were conducted with 5 min intervals between each trial. Paw withdrawal thresholds were calculated as the mean of the two values.
Animals were randomised and allocated to treatment groups to achieve a minimum statistical power of 80%. In all cases the experimenter was blind to the treatment received.
*Collection of plasma for determination of compound levels in behavioral assay*: A separate group of naïve rats, satellite animals, not subjected to nociceptive testing were used for plasma collection in order to establish the PK/PD relationship. At the appropriate time point, satellite animals were injected with drug using the same dosing solution and route of administration as the tested animals. Blood was collected by decapitation. Whole blood was transferred to heparinized tubes and centrifuged at 3000*g* for 5 min. Plasma supernatant was then collected and frozen (−80 °C). The measurement of compound concentration was carried out on a generic HPLC coupled to a mass spectrometer with an electrospray ionization source in the positive mode using multiple reaction monitoring. Chromatographic separations were performed using a generic reverse phase HPLC C18 column (2.1 × 50 mm, 3 μ). The mobile phase consisted of 0.1% formic acid in purified water (solvent A) and 100% acetonitrile containing 0.1% formic acid (solvent B). The following gradient was used: 5% to 95% solvent B in 2 min. The flow rate was constant at 0.750 mL/min and the column temperature was set at 45 °C. Data processing was performed using the LC/MS/MS software. Rat plasma protein binding was determined in vitro using an equilibrium dialysis technique run at 10 μM. [Kalvass, J.C.; Maurer, T.S. Biopharmaceutics Drug Disposition **2002**, *23*, 327–338.] The degree of brain binding was assessed by equilibrium dialysis and samples were analyzed by LC–MS/MS.
*Data analysis*: Data are presented as a mean data ± SEM. Statistical significance was determined using one-way measures ANOVA followed by a Holm-Sidack post hoc test using SigmaStat statistical package (Systat Software Inc., ver. 3.11). A *p*-Value of less than 0.05 was regarded as significant. Free plasma $EC_{50}$ values in behavioral studies were determined from 4-point concentration-response curves using non-linear regression and a sigmoidal variable slope logistic model (Prism 4.03, GraphPad Software Inc., USA).
15. We synthesized a number of enantiomeric pairs, and in all cases the *S*-enantiomer was the only one active. The *R*-enantiomer was consistently inactive.
16. (a) Huang, L.; Berry, L.; Ganga, S.; Janosky, B.; Chen, A.; Roberts, J.; Colletti, A. E.; Lin, M.-H. J. *Drug Metab. Dispostion* **2010**, *38*, 223; (b) Harrison, A.; Betts, A.; Fenner, K.; Beaumont, K.; Edgington, A.; Roffey, S.; Davis, J.; Comby, P.; Morgan, P. *Drug Metabo. Disposition* **2004**, *32*, 197.